Electronic Supplementary Information

First-principles study of pressure-induced phase transformation in a rare-earth formate framework

Soumya S. Bhat,[a] Wei Li,[b] Anthony K. Cheetham,[c] Umesh V. Waghmare,[d] and Upadrasta Ramamurty[a,e]

[a]*Department of Materials Engineering, Indian Institute of Science, Bangalore 560012, India.*

[b]*School of Physics, Huazhong University of Science and Technology, Wuhan, China.*

[c]*Department of Materials Science & Metallurgy, University of Cambridge, Cambridge CB3 0FS, UK.*

[d]*Theoretical Science Unit, Jawaharlal Nehru Centre for Advanced Scientific Research, Jakkur, Bangalore 560064, India.*

[e]*Centre for Excellence for Advanced Materials Research, King Abdulaziz University, Jeddah 21589, Saudi Arabia.*

1. Preliminary calculations

As a first step, starting with the optimized ambient pressure phase I structure, we have carried out variable-cell relax calculation with different target pressures. This is achieved in three ways, (i) Atomic positions of phase I structure at ambient pressure is used as input structure with scaled experimental cell parameters. Scaling factor is determined as the ratio of calculated lattice constant to the experimental lattice constant, at ambient pressure. For example, for target pressure P,

$$a_{input}(P) = r \times a_{\mathrm{exp}t}(P),$$

where, $r = \left(a_{calc} \big/ a_{\mathrm{exp}t} \right) \Big|_{P=0\ \mathrm{GPa}}$,

Method-1 hereafter, (ii) Optimized phase I structure is used as input, with cell parameters same as that of ambient structure, Method-2 hereafter, and (iii) Atomic positions of optimized phase I structure at ambient pressure is used as input with experimental cell parameters corresponding to the target pressure (Method-3). The results are summarized in Table S1. Even after the application of pressure as high as 8 GPa, PIPT is not observed and the final structure retained the bonding characteristics of phase I.

Table S1. Calculated lattice constants (in Å), monoclinic angle (in °) and volume (in $Å^3$) of the unit cell for phase I at different pressures (in GPa) along with experimental values.

Pressure		Method-1	Method-2	Method-3	Experiment[a]
0	*a*		14.89		14.74
	b		13.17		13.00
	c		12.99		12.78
	β		105.6		105.0
	V		2451		2366
1.1	*a*	14.22	14.63	13.69	13.13
	b	13.05	13.09	13.04	13.05
	c	12.91	12.87	12.98	12.85
	β	105.6	105.9	105.1	105.7
	V	2306	2370	2236	2118
2.0	*a*	13.81	14.35	13.71	13.03
	b	12.96	12.98	12.92	12.93
	c	12.83	12.79	12.80	12.75
	β	105.7	106.4	105.6	105.4
	V	2209	2286	2182	2071
2.7	*a*	13.66	14.16	13.56	12.92
	b	12.86	12.92	12.81	12.85
	c	13.32	12.72	12.76	12.70
	β	105.5	106.5	105.3	105.1
	V	2162	2232	2139	2037
3.5	*a*	13.75	13.93	13.43	12.84
	b	12.75	12.79	12.69	12.73
	c	12.68	12.66	12.70	12.63
	β	105.6	106.4	104.8	104.4
	V	2140	2164	2091	1998
8.0	a		12.99		
	b		12.23		
	c		12.49		
	β		105.7		
	V		1910		

[a] Supporting data Table S2 of reference[1].

2. Phase II at P=0 GPa

Starting with the phase II structure measured at 3.5 GPa, we have carried out variable-cell relax calculation with P=0 GPa and the results are presented in Table S2. The resulting optimized structure retained the bonding characteristics of phase II.

Table S2. Calculated lattice constants (in Å), monoclinic angle (in °) and volume (in Å^3) of the unit cell for phase II at P=0 GPa.

	Phase II
a	13.25
b	13.16
c	13.02
β	104.9
Volume	2193

3. Results of DFT-D2 calculation

Table S3. Calculated lattice constants (in Å), monoclinic angle (in °) and volume (in Å^3) of the unit cell for phase I at ambient pressure and phase II at 3.5 GPa, using DFT-D2 calculations. Corresponding experimental[a] values are given in parentheses.

	Phase I	Phase II
a	14.45 (14.72)	12.62 (12.77)
b	13.01 (12.99)	12.55 (12.75)
c	12.74 (12.77)	12.70 (12.64)
β	106.1 (105.0)	103.8(104.6)
Volume	2303 (2358)	1953 (1991)

[a] Table S1 of reference[1].

The energy difference between phases II and I is 49.1 kJ/mol (0.51 eV/f.u.), which is comparable to that obtained using calculations performed without dispersion interactions.

4. Energy as a function of volume for both phases I and II

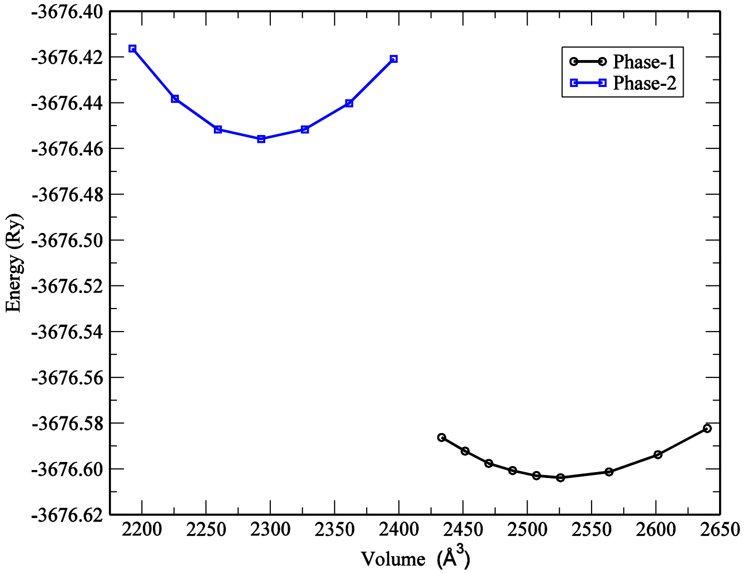

Fig. S1 Energy as a function of volume for Phases I and II of framework 1.

5. Electronic density of states

Fig. S2 shows calculated electronic density of states of phases I and II. For both phases the states below the Fermi level, E_f are dominated by hybridized C 2p and O 2p states. The electronic states near E_f are due to O 2p states, with slightly stronger covalency in phase II, as reflected in its broader bands. It is evident from Fig.S2 that there are no significant differences in the electronic states near the gap of phases I and II, indicating marginal changes in the electronic properties across the phase transition. Like most rare-earth carboxylate MOFs, both phases are expected to be insulators.

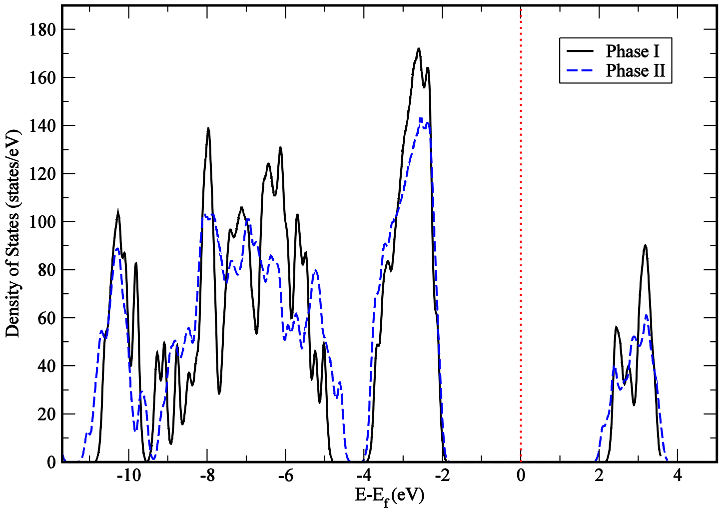

Fig. S2 Electronic density of states of framework 1 for phases I and II. The Fermi level is set at zero energy and marked by a vertical line.

References

1 E. C. Spencer, M. S. R. N. Kiran, W. Li, U. Ramamurty, N. L. Ross and A. K. Cheetham, *Angew. Chemie Int. Ed.*, 2014, **53**, 5583–5586.

2 S. Grimme, *J. Comput. Chem.*, 2006, **27**, 1787–1799.